Elsevier Editorial System(tm) for Protein Expression and Purification
Manuscript Draft

Manuscript Number:

Title: Cloning and heterologous overexpression of three gap genes encoding different glyceraldehyde-3-phosphate dehydrogenases from the plant pathogenic bacterium Pseudomonas syringae pv. tomato strain DC3000

Article Type: Regular Article

Keywords: Pseudomonas syringae pv tomato DC3000,
Glyceraldehyde-3-phosphate dehydrogenase (GAPDH),
Paralogous gap genes,
Heterologous protein,
Optimized overexpression.

Order of Authors: Bouchra Elkhalfi, PhD; José Miguel Araya, PhD; Jorge Rodríguez Castro, PhD; Manuel Rey Méndez, Dr; Abdelaziz Soukri, Dr; Aurelio Serrano, Dr

Abstract: The gammaproteobacterium Pseudomonas syringae pv. tomato DC3000 is the causal agent of bacterial speck, a common disease of tomato. The mode of infection of this pathogen is not well understood, but according to molecular biological, genomic and proteomic data it produces a number of proteins that may promote infection and draw nutrients from the plant. Glyceraldehyde-3-phosphate dehydrogenase (GAPDH) is a major enzyme of carbon metabolism that was reported to be a surface antigen and virulence factor in other pathogenic microorganisms, but its possible role in the infection process of P. syringae has so far not been studied. Whole-genome sequence analyses revealed the occurrence in this phytopathogenic bacterium of three paralogous gap genes encoding distinct GAPDHs, namely two class I enzymes having different molecular mass subunits and one class III bifunctional D-erythrose-4-phosphate dehydrogenase/GAPDH enzyme. By using genome bioinformatics data, as well as alignments of both DNA and deduced protein sequences, the three gap genes of P. syringae were one-step cloned with a His-Tag in pET21a vector using a PCR-based strategy, and its expression optimized in E. coli BL21 to achieve high yield of the heterologous proteins. In accordance with their distinct molecular phylogenies, these bacterial gap genes encode functional GAPDHs of diverse molecular masses and nicotinamide-coenzyme specificities, suggesting specific metabolic and/or cellular roles.

***Highlights (for review)**

-Whole-genome sequence analyses revealed the occurrence in the phytopathogenic bacterium *Pseudomonas syringae* pv. tomato DC300, of three paralogous *gap* genes encoding distinct GAPDHs, namely two class I enzymes having different molecular mass subunits and one class III bifunctional D-erythrose-4-phosphate dehydrogenase/GAPDH enzyme.

-By using genome bioinformatics data, as well as alignments of both DNA and deduced protein sequences, the three *gap* genes of *P. syringae* were one-step cloned with a His-Tag in pET21a vector using a PCR-based strategy.

-We optimized their expression in *E. coli* BL21 to achieve high yield of the heterologous proteins.

-In order to verify a possible toxic character of *P. syringae* GAPDH2 on the *E. coli* BL21 host cells, a comparative study was performed concerning the effect of different alternatives carbon sources (glucose, glycerol, succinate, succinate *plus* glycerol) on the overproduction of the heterologous GAPDHs.

-The 36-kDa GAPDH1 band follows the expected pattern for T7-lac promoter-dependent production, namely, heterologous protein decrease by glucose (actually an inhibitor of T7-lac-promoter transcription).

-The 52-kDa GAPDH2 band shows a clear increase in the presence of glucose and reduction with succinate and/or glycerol. This finding suggests stabilization of pET21a-*gap2* construct by glucose, which is a characteristic feature of the heterologous expression of toxic proteins in *E. coli.*

-In accordance with their distinct molecular phylogenies, these bacterial *gap* genes encode functional GAPDHs of diverse molecular masses and nicotinamide-coenzyme specificities, suggesting specific metabolic and/or cellular roles.

Protein Expr Purif. 2013 Jun;89(2):146-55. doi: 10.1016/j.pep.2013.02.005

Cloning and heterologous overexpression of three *gap* genes encoding different glyceraldehyde-3-phosphate dehydrogenases from the plant pathogenic bacterium *Pseudomonas syringae* pv. tomato strain DC3000

Bouchra Elkhalfi[1], José Miguel Araya-Garay[2], Jorge Rodríguez Castro[2], Manuel Rey Méndez[2], Abdelaziz Soukri[1], Aurelio Serrano[3]

[1] Laboratory of Physiology & Genetics Molecular. Faculty of Sciences Ain Chock, Casablanca Morocco,

[2] Laboratory of Molecular Systematic. CIBUS University of Santiago de Compostela, Santiago de Compostela, Spain,

[3] Institute for Plant Biochemistry and Photosynthesis (CSIC-University. Of Seville), Seville, Spain,

Corresponding Authors:

Abdelaziz SOUKRI: a_soukri@hotmail.com

00212661095495

Faculty of Sciences Ain Chock,Km8 Route Eljadida B;P 5366 Maarif, Casablanca 20100 Morocco

Abstract:

The gammaproteobacterium *Pseudomonas syringae* pv. tomato DC3000 is the causal agent of bacterial speck, a common disease of tomato. The mode of infection of this pathogen is not well understood, but according to molecular biological, genomic and proteomic data it produces a number of proteins that may promote infection and draw nutrients from the plant. Glyceraldehyde-3-phosphate dehydrogenase (GAPDH) is a major enzyme of carbon metabolism that was reported to be a surface antigen and virulence factor in other pathogenic microorganisms, but its possible role in the infection process of *P. syringae* has so far not been studied. Whole-genome sequence analyses revealed the occurrence in this phytopathogenic bacterium of three paralogous *gap* genes encoding distinct GAPDHs, namely two class I enzymes having different molecular mass subunits and one class III bifunctional D-erythrose-4-phosphate dehydrogenase/GAPDH enzyme. By using genome bioinformatics data, as well as alignments of both DNA and deduced protein sequences, the three *gap* genes of *P. syringae* were one-step cloned with a His-Tag in pET21a vector using a PCR-based strategy, and its expression optimized in *E. coli* BL21 to achieve high yield of the heterologous proteins. In accordance with their distinct molecular phylogenies, these bacterial *gap* genes encode functional GAPDHs of diverse molecular masses and nicotinamide-coenzyme specificities, suggesting specific metabolic and/or cellular roles.

Key words: *Pseudomonas syringae* pv tomato DC3000, glyceraldehyde-3-phosphate dehydrogenase, GAPDH, paralogous *gap* genes, heterologous protein; optimized overexpression

Abbreviations: GAPDH, glyceraldehyde-3-phosphate dehydrogenase; IPTG, isopropyl-β-D-thiogalactopyranoside; LB, Luria-Bertani; PCR, Polymerase Chain Reaction; SDS-PAGE, sodium dodecyl sulfate polyacrylamide gel electrophoresis.

Introduction

Tomato is an outstanding crop grown in many countries around the world and under diverse climates, including relatively cold regions, due to the development of vegetable crops under cover. By the volume of its production, tomato remains the first vegetable in the world [1,2]. However, tomato fields are potential targets of pathogenic bacteria that cause diseases ranging from small spots on the foliage to the almost total defoliation of the plant, with severe consequences on photosynthesis and yield potential [3,4] One of these diseases is bacterial speck caused by the gram-negative bacteria strain *Pseudomonas syringae* pv. tomato DC3000, a member of the gamma subgroup of the Proteobacteria[5]. This bacterium has emerged as an important model organism in molecular plant pathology because of its genetic tractability, and its genome has been fully sequenced [6,7]. *P syringae* pv. Tomato DC3000 causes leaf lesions characterized by small brown-black specks, 1-3 mm in diameter, with a yellow chlorotic halo [8], and it can survive up to 20 years in the crevices and cavities of the tomato seed coat. These lesions constitute a severe blemish on fruit for fresh market and greatly reduce yield potential [9].

Up to now, the virulence molecular mechanisms of *P. syringae* are not well understood. Previous research reported that this strain encodes a wide range of proteins that are involved in virulence, and 298 genes (ca. 5 % of the total) have been identified in the virulence category [7]. One of these proteins is glyceraldehyde-3-phosphate dehydrogenase (GAPDH), a highly conserved enzyme during evolution with a key role in the glycolytic and gluconeogenic pathways. GAPDH catalyzes the redox-linked reversible phosphorylation of glyceraldehyde-3-phosphate to 1,3-diphosphoglycerate, in the presence of $NAD(P)^+$ and inorganic phosphate [10]. GAPDH family members are classified into the ubiquitous class I enzymes that utilize NAD^+ (EC 1.2.1.12), $NADP^+$ (EC 1.2.1.13) or either (EC 1.2.1.59), class II of archaeal $NAD(P)^+$-dependent GAPDHs, and class III bifunctional enzymes (erythrose-4-phosphate dehydrogenase/GAPDH) that are prevalent among gamma-proteobacteria [11]. Most glycolytic class I GAPDHs so far studied are homotetrameric proteins with 34–38 kDa subunits, and the native oligomer has a molecular weight of 140-150 kDa [12–14]. In addition to its classic metabolic roles, GAPDH has been claimed to be involved in a number of diverse cellular processes unrelated to glycolysis ("moonlighting protein"). Many of these alternative roles are dependent on the ability of GAPDH to modify its subcellular localization. In particular, it has been reported to bind DNA and RNA [15,16] and regulate transcription in cell nuclei [17,18], to exhibit kinase/phosphotransferase activity [19], to catalyze microtubule formation thus facilitating vesicular transport, and to bind to membrane-associated ion pumps involved in Ca^{2+} release. Besides, it interacts with a number of small molecules, including tumor necrosis α-factor, ribozymes, glutathione and nitric oxide [20]. Since GAPDH interacts with disease-associated proteins, like huntingtin [21] and the amyloid β-protein precursor [22], it also operates as a fusogenic protein in rabbit brain cytosol [23] and in nuclear membrane assembly in *Xenopus* eggs [24]. On the other hand, a functional GAPDH has

been reported as a cell wall component in yeasts, like *Saccharomyces cerevisiae*[25]. Usually, GAPDH was used as a model protein, or control, in gene regulation and catalytic mechanism related studies, as well as a standard in Northern and Western blots, because of its high degree of structural conservation across species [18]. Furthermore, despite its general consideration as a housekeeping enzyme, GAPDH recently emerged with the advent of the molecular biotechnology as a useful model for innovative methods to advance our understanding of the mechanisms through which cells organize and express their genetic information [26]. Regarding its role in some pathogenic organisms, the presence of a surface-associated GAPDH has been reported on all streptococcal strains tested so far (21), as well as in microorganisms as diverse as *Candida albicans*, *Schistosoma bovi*s, *Mycoplasma genitalium*, and *Staphylococcus* spp. [27]. GAPDH was shown to be secreted by several pathogenic bacteria, like *Streptococcus pyogenes* and a number of enteropathogenic *Escherichia coli* strains [28–30]. It was claimed that secreted GAPDH has a role in signal transduction to their host cells, rendering them probably more susceptible to bacterial infection [28,31]. Three GAPDH encoding genes are present in the genome of *P. syringae* pv. tomato DC3000 [5,7]. It remains to be established whether any of these bacterial GAPDHs are extracellular proteins involved in the plant infection process. Their possible secretion and association to the cell membrane might have biotechnological implications that are worth to be further investigated.

In the present work, we successfully cloned and optimized overexpression in *E. coli* of three paralogous *gap* genes encoding different GAPDHs identified in the genome of *Pseudomonas syringae* pv. tomato DC300. Some molecular and catalytic parameters of the recombinant GAPDHs of this phytopathogenic bacterium have been determined revealing the diverse structural and functional features of these enzymes.

Materials and Methods

Bioinformatics research: search, alignment and sequences analysis

Searches for sequences of *gap* genes in EMBL/DDBJ/GeneBank databases, and multiple alignments of GAPDH sequences, were performed using the bioinformatics programs Blast and Clustal X v.2.0, respectively. Domain structures of the predicted proteins were analyzed with the ProDom (http://prodom.prabi.fr/prodom/current/html/home.php), SUPERFAMILY (http://supfam.cs.bris.ac.uk/SUPERFAMILY/) and Pfam (http://pfam.sanger.ac.uk/) bioinformatics tools

Organisms and growth conditions

P. syringae was cultured in LB medium with glucose (3 g/l) at 28 °C in the presence of rifampicin (50 µg/ml) with agitation (200 rpm) in the dark. Unless otherwise indicated, *E. coli* Top10 and BL21 strains were grown in LB medium at 37 °C with agitation (200 rpm), and ampicillin was employed for selection of transformants. Where indicated, an additional carbon source -glycerol, succinate or glucose- was added at a final concentration of 2 % (w/v) to the LB medium. When necessary,

ampicillin and isopropyl-β-D-thiogalactopyranoside (IPTG) were added at concentrations of 50-100 µg/ml and 1 mg/ml, respectively.

DNA manipulation and cloning strategy

-*DNA isolation and purification.* A modified phenol-chloroform method was used for the extraction of chromosomal DNA from *Pseudomonas syringae* pv. tomato DC3000 cells. Purified DNA was eventually washed with 70% (v/v) ethanol, air dried and resuspended in 100-200 µl of TE buffer. DNA concentration was estimated after 100-fold dilution in 1 ml of TE and measuring ultraviolet absorbance at 260 nm.

-*Primers Design.* Specific primers for each putative *gap* gene of *P. syringae* were designed using Primer Premier 5.0 (Biosoft International). At each primer end, a new restriction site was added as shown in Table 1 to facilitate directional cloning.

-*Cloning strategy*

Step 1. *Amplification by PCR.* To check primers, a PCR amplification of the complete open reading frames (ORF) of the three *gap* genes was carried out with their specific complementary oligonucleotides, using the genomic DNA from *P. syringae* pv tomato as a template. The reaction mixture contained 100 mM Tris-HCl buffer (pH 8.3), 1.5 mM $MgCl_2$, 0.8 mM of each deoxynucleoside triphosphate, 0.08 µM of each primer, 50 ng of DNA, and 1 U of *GoTaq* DNA Polymerase (Promega). Amplification was performed in a DNA thermal cycler (Perkin–Elmer Cetus, Norwalk, CT) programmed for 2 min at 95 °C and 35 cycles of 40 s at 94 °C, 40 s at 60 °C, and 1 min at 72 °C. In the end, a final cycle of 7 min at 72 °C was added. In this way, new restriction sites were created to facilitate directional one-step cloning of the amplified DNA fragments. Amplification products were resolved by electrophoresis in a 0.8% agarose gel according to Sambrook [32] and detected by staining with ethidium bromide. After agarose gel electrophoresis the PCR-amplified DNA fragments were purified with Wizard SV Gel and PCR Clean-Up System kits (Promega).

Step 2. *Digestion of inserts and plasmid, and ligation.* The plasmid pET-21a (Novagen, Cambridge, UK) and the three PCR-amplified DNA fragments (1-1.5 kb) were sequencially cleaved, first with *Nde*I endonuclease overnight and purified; then, the second cleavage was carried out also overnight by *Bam*H1 for plasmid pET-21a and the *gap1* and *gap3* inserts, or by *Hind*III for plasmid pET-21a and the *gap2* insert. The reaction mixtures were carried out according to the manufacturer's recommendations of each restriction enzyme. All DNA ligations were carried out with T4 DNA ligase (New England BioLabs, MA), as recommended by the manufacturer. Ligation reactions between the vector and the inserts were analyzed by PCR using T7 vector-specific primers and a combination of vector-specific and insert-specific primers.

Step 3. *Transformation into non-expressing host E. coli Top10.* After DNA ligation, recombinant plasmids were transformed into chemically-competent *E. coli* Top 10 "One shot" (Invitrogen), which

was grown on low salt LB agar plates containing 50 μg/ml ampicillin. Plates were then incubated overnight at 37 °C and recombinant colonies were selected.

Step 4. *Colony PCR and sequencing.* Before growing colonies for plasmid isolation, subcloning was verified by analyzing the presence of the appropriate insert and its orientation by single-colony PCR using T7 vector-specific primers and a combination of vector-specific and insert-specific primers. Then, plasmids were isolated by E.Z.N.A R Plasmid Mini Kit I, and reading frame verified by sequencing.

Step 5. *Heterologous expression by transformation into host E. coli BL21 and induction.* Recombinant pET-21a (Novagen, Cambridge, UK) expression vectors containing the complete ORF of each *P. syringae gap* gene (pET21a-*gap1*, pET21a-*gap2* and pET21a-*gap3*) was transformed into *E. coli* BL21 (DE3) (Invitrogen) and grown on low-salt LB media containing 50 μg/ml ampicillin, until cultures reached an OD of 0.5–1. The cultures were then inducted by addition of IPTG. After four hours and overnight incubation at 37 or 22 ℃, cells were harvested by centrifugation at 4 °C (8,000 ***g***, 10 min). Cell pellets were washed twice in 25 mM Tris–HCl buffer, pH 7.5, and resuspended in the same buffer supplemented with 2 mM EDTA, 1 mM phenylmethylsulfonyl fluoride (PMSF), and 10% (v/v) glycerol. The cells were then disrupted by sonication in a chilling water bath, using a Branson model B12 Sonifier at medium strength. The resulting broken-cell suspension was centrifuged at 20,000 *g* for 30 min at 4 ℃ to obtain the soluble protein fraction, or crude extract.

Protein techniques

Protein concentration was estimated by the Bradford technique [33], using ovalbumin as a standard.

-*Protein electrophoresis (SDS-PAGE)*. Prior to polyacrylamide gel electrophoresis, samples were incubated at 100 °C for 3min in solubilization buffer containing 2.5 % (w/v) SDS, 125 mM dithiothreitol, 25 % (v/v) glycerol and 112.5 mM Tris–HCl, pH 6.8. The protein samples were then loaded onto a 12 % polyacrylamide gel and separated on a Mini Protean II cell (Bio-Rad, Hercules, CA), according to the method of Laemmli [34].

The gel was run at 120 V for 1 h, using Tris–Glycine buffer (25 mM Tris; 192 mM Glycine; 0.1 % SDS; pH: 8.3). The molecular mass of the proteins was estimated using Precision Plus Protein Standard (Bio-Rad) and the analysis software Quantity One (Bio-Rad). Western blots after SDS-PAGE and transfer to nitrocellulose membranes were carried out as previously described[35].

-*Enzyme assays*. The phosphorylating GAPDH activity was measured spectrophotometrically, using a Jenway 6405 UV/Visible spectrophotometer (Bibby Scientific Ltd, Stone, UK). The reaction was started by adding the enzyme preparation to the assay mixture containing 50 mM Tricine buffer (pH 8.5), 10 mM sodium arsenate (AsO_4^{3-}), 1mM NAD^+ or $NADP^+$, and 2 mM D-glyceraldehyde-3-phosphate (D-G3P) at 25 °C, The total volume of the reaction mixture was 1 ml. Absorbance changes at 340 nm were monitored. One unit of enzyme (U) was defined as the amount that catalyzes the

reduction of 1 µmol of NAD^+ or $NADP^+$ per minute. All experiments and assays were carried out in triplicate.

Results and discussions

Occurrence of three distinct paralogous gap genes of diverse molecular phylogeny in P. syringae pv. tomato DC3000

Bioinformatic searches in databases identified three putative *gap* genes that encode distinct GAPDH proteins and are located in different regions of the *P. syringae* pv. tomato DC3000 genome: PSPTO_1287 (gi|28868497), PSPTO_2102 (gi|28869306), and PSPTO_0386 (gi|28867616), which were named as *gap1*, *gap2* and *gap3*, respectively.

Gap1 gene encodes a class I glyceraldehyde-3-phosphate dehydrogenase (GAPDH1) of 333 aminoacids, with a predicted molecular mass and a p*I* value of 36,260 Da and 6.22, respectively. These are the expected values for archetypical glycolytic-gluconeogenic GAPDHs. The two structural domains proper of GAPDHs, namely NAD(P)-binding Rossmann-fold and C-terminal GAPDH domain were clearly identified by using several structural bioinformatics tools (Figure 1). This gene takes place in the genome of *P. syringae* near to genes encoding a 6-phosphogluconate dehydratase (*edd*), a RNA polymerase sigma70 factor (PSPTO_1286), a glucokinase (*glk*), a glucose transporter, permease proteins and several hypothetical proteins (Figure 2). It should be noted that adjacent divergent genes *gap1* and *edd* (involved in the same KEGG metabolic pathways) arrange in a head-to-head manner in opposite orientations suggesting regulation by a single bidirectional promoter. This genomic organization is conserved in most *Pseudomonas* strains (both pathogenic and non-pathogenic), and other gammaproeobacteria (e.g. *Marinobacter* sp. *Chromohalobacter salexigens*, and *Marinomonas* spp.). However, *gap1* appears in an operon with *edd* and a pyruvate kinase (*pyk*) encoding gene in other gammaproteobacteria (e.g. *Nitrosococcus watsoni*, *Marinobacter* spp.).

It is interesting to note that two protein spots have been identified as GAPDH1 (PSPTO_1287) in 2D-PAGE gels of the extracellular proteins of *P. syringae* pv. tomato DC3000, showing a virtually identical *pI* but different molecular masses (http://www.leelab.org/wildtype_extracellular.html, Dr. Kelvin Lee's Research Group, Delaware Biotechnology Institute, University of Delaware, USA;).

This result, obtained in a massive proteomic study, strongly suggests that two GAPDH isoforms generated by post-translational modification are secreted by this bacterium, although no detailed studies on this subject have been performed so far. A similar scenario has been reported for pathogenic *E. coli* strains, namely GAPDHA is secreted to the periplasmic compartment and the extracellular medium [29,30]. Moreover, post-translational modification of the secreted GAPDH has been described in the parasitic protist *Entamoeba histolytica* [36].

Gap2 gene encodes a class I glyceraldehyde-3-phosphate dehydrogenase (GAPDH2) of 482 aminoacids, with a predicted molecular mass and a p*I* value of 52,733 Da and 6.94, respectively. This

comparatively higher molecular mass is due to the presence of an additional N-terminal sequence of ca. 130 residues without specific structural features upstream of its GAPDH-specific domains (Figure 3), so the encoded polypeptide is larger than a canonical class I GAPDHs (ca. 36 kDa). This non-conventional GAPDH presents high homology to a select group of bacterial GAPDHs weakly inhibited by high ATP concentrations, which have been suggested to participate in the gluconeogenic pathway [37]. This *gap* gene takes place in the genome of *P. syringae* near to genes encoding a transcription-repair coupling factor (*mfd*), a helicase (PSPTO_2099), a hypotetical protein (PSPTO_2103), a major facilitator family transporter (PSPTO_2104), and a lysozyme putative reductase family (Figure 4). Adjacent divergent genes *gap2* and *mfd* arrange in a head-to-head manner in opposite orientations suggesting regulation by a single bidirectional promoter, in a genomic scenario similar to that previously described for *gap1*. This genomic organization is conserved in all *Pseudomonas* strains analyzed so far (both pathogenic and non-pathogenic), as well as in other gammaproeobacteria (e.g. *Azotobacter vinelandii*, *Chromohalobacter salexigens*, *Halomonas* spp., *Marinobacter* spp. and *Oceanospirillum* spp.). Although in most cases *gap2* is not included in operons, in some *Pseudomonas* strains (e.g. *P. aeruginosa* and *P. stutzeri*) and in other gammaproteobacteria (e.g. *Alcanivorax* sp., *Marinobacter* spp.) it appears upstream of a cluster of *nqr* genes encoding different subunits of a Na^+-translocating NADH:ubiquinone oxidoreductase (data not shown).

Gap3 gene encodes, a putative class III bifunctional enzyme of 347 aminoacids (GAPDH3, D-erythrose 4-phosphate dehydrogenase /G3P dehydrogenase) with a predicted molecular mass and a p*I* value of 38,317 Da and 5.94, respectively. The two structural domains proper of GAPDHs, namely NAD(P)-binding Rossmann-fold and C-terminal GAPDH domain were identified by several structural bioinformatics tools (Figure 5). This protein shows a high homology to a family of eubacterial orthologs with dual substrate specificity, prevailing among gammaproteobacteria [38]. In the genome of *P. syringae* pv. tomato str. DC3000 the *gap3/epd* gene is part of an operon that includes genes of other key enzymes of central carbon metabolism (glycolysis, pentoses-phosphate pathway): namely transketolase (*tkt*), upstream, and phosphoglycerate kinase (*pgk*) and fructose-bisphosphate aldolase (*fba*), downstream (Figure 6). This is an expected genomic organization since class III GAPDHs, which exhibit a high homology with typical catabolic class I GAPDHs, can functionally replace them and perform a catabolic role. This genomic organization is remarkably conserved in all *Pseudomonas* strains analyzed so far and in many other gammaproteobacteria (e.g. the *gapB/epd-pgk-fba* operon of *Escherichia coli*). This is in sharp contrast to the scenario in other main bacterial groups, in which *gap1* is located upstream *pgk* in an operon of genes encoding glycolytic/gluconeogenic enzymes [39].

Summarizing, bioinformatics sequence analyses showed that three *gap* genes located in distant regions with different genomic organization occur in the 6.5-Mb chromosome of *P. syringae* pv. tomato DC300, namely at ca. 1.41 (*gap1*), 2.28 (*gap2*) and 0.43 (*gap3*) Mb from the replication origin.

Moreover, these paralogous genes are predicted to encode GAPDH proteins with distinct molecular and catalytic features. To confirm this proposal, the *P. syringae* pv. tomato DC3000 genes have been cloned, overexpressed, and optimized for the production of functional heterologous proteins in *E. coli*.

Multiple sequence alignment of the GAPDHs encoded by the three *gap* genes of *Pseudomonas syringae* pv tomato DC3000, generated by both Cobalt and Clustal (v. W2 and X) programs, showed high levels of structural conservation between these proteins, although it was highest between GAPDH1 and GAPDH2, and conservation of amino acid residues essential for enzymatic activity (Figure 7).

Proteins encoded by *gap1* and *gap3* are, respectively, clear orthologs of the canonical class I glycolytic/gluconeogenic GapA, with orthologs in many bacteria and eukaryotes, and the class III GapB/Epd bifunctional enzyme of *E. coli*, also found in many other gammaproteobacteria and in other (alpha, beta and delta) proteobacterial groups (see below). The *gap2* encoded enzyme (GAPDH2) belongs to a definite subgroup of ATP-insensitive class I GAPDHs of larger 50-kDa subunits (with an extra N-terminal region) found so far in gammaproteobacteria (all *Pseudomonas* strains) and in some other bacterial groups, i.e. actibacteria, like *Corynebacteium glutamicum* [37]. It is interesting to note that these three gap genes are also present in the genome of other pathovars of P. syringae, as discussed below. The phylogenic relationships of P. syringae pv. tomato DC3000 GAPDHs with other selected bacterial and eukaryotic GAPDHs are shown in Figure 8 and strongly suggest specific metabolic/cellular roles for these bacterial GAPDH paralogs. Therefore, further work is needed to clarify the physiological roles of these enzymes in this pathogenic bacterium.

Cloning and overexpression of the three gap genes of P. syringae pv. tomato DC3000 and optimized production of functional GAPDHs in E. coli BL21 cells

The coding region of each *gap* gene was amplified by PCR using *P. syringae* chromosomal DNA as a template with sets of specific primers containing engineered restriction sites, *Bam*HI and *Nde*I restriction sites for *gap1*and *gap3*, and *Hind*III and *Nde*I for *gap2* (Figure 9). These primers were selected after analyzing the genome sequence (Gen-Bank database http://www.ncbi.nlm.nih.gov), and designed using Primer Premier 5.0 tool (Biosoft International). Specific restriction sites added to each primer at their 5' and 3' ends allowed directional cloning of the insert containing each *P. syringae gap* gene directly into the expression vector pET21a, without passing through pGEM-T cloning (see Table of primers, Material and Methods). PCR products were cleaved with NdeI–BamHI endonucleases for *gap1* and *gap3*, and NdeI–HindIII endonucleases for *gap2*. Then, each cleaved DNA fragment was ligated into pET21a vector previously cleaved with the same specific endonucleases to generate the final constructs.

A ligation reaction between the expression vector and each insert was analyzed by PCR using T7 vector-specific primers and a combination of vector-specific and insert-specific primers. The product

of each ligation was transformed into non-expression host Top10 strain. Sub-cloning was verified by analyzing the presence of the appropriate insert and its orientation by colony-PCR, using T7 vector-specific primers and a combination of vector-specific and insert-specific primers. Then, correct reading frame was verified for each construct by clone sequencing after plasmid isolation.

Verified plasmids containing the complete ORF of each *gap* gene were eventually transformed into expression host *E. coli* BL-21, and cell-free extracts obtained as described above. Induction was carried out with IPTG during 4h or overnight, as described in Material and Methods, and overproduction of recombinant proteins was subsequently checked in cell-free extracts (soluble protein fraction) by both SDS-PAGE and GAPDH activity tests (see below).

However, significant differences were observed in the culture conditions required for optimal overproduction of the three different *P. syringae* GAPDHs in *E. coli* BL21 cells. SDS–PAGE analysis of total protein preparations from *gap1*- and *gap2*-transformed clones show a conspicuous band of the corresponding recombinant protein (ca. 36 or 52 kDa) specifically after overnight or 4 h IPTG induction, respectively (Fig. 10). This result suggests that GAPDH2 should be to some extent toxic for *E. coli* BL21 cells. On the other hand, optimal overproduction of the 38-kDa GAPDH3 protein was achieved specifically after overnight IPTG induction at 22 ºC. At the standard growth temperature for *E. coli* (37º C) most recombinant GAPDH3 was recovered as inclusion bodies in the insoluble protein fraction (data not shown). No protein bands corresponding to the heterologous proteins were observed in non-transformed *E. coli* BL-21 and in uninduced BL-21 (pET21a) strain (see Fig. 10).

In order to verify a possible toxic character of *P. syringae* GAPDH2 on the *E. coli* BL21 host cells, a comparative study was performed concerning the effect of different alternatives carbon sources (glucose, glycerol, succinate, succinate *plus* glycerol) on the overproduction of the heterologous GAPDHs. As it was shown by SDS-PAGE (Figure 11), the 36-kDa GAPDH1 band follows the expected pattern for T7-lac promoter-dependent production, namely, heterologous protein decrease by glucose (actually an inhibitor of T7-lac-promoter transcription). On the contrary, the 52-kDa GAPDH2 band shows a clear increase in the presence of glucose and reduction with succinate and/or glycerol (see Fig. 11). This last scenario suggests stabilization of pET21a-*gap2* construct by glucose, which is a characteristic feature of the heterologous expression of toxic proteins in *E. coli* [40]

It is interesting to note that monospecific antibodies against the glycolytic GapC ortholog of the protist *Tetrahymena pyrofirmis* [41] weekly detected in *E. coli* BL21 extracts both overproduced recombinant GAPDH1 (class I) and GAPDH3 (class III) proteins, but could not detect the 50-kDa class I GAPDH2 (Figure 12, left panel). On the other hand, polyclonal antibodies obtained in rabbit against the recombinant GAPDH2 (Elkahlfi B. et al, unpublished results) specifically recognizes its 50-kDa polypeptide in cell extracts of *gap2*-transformed BL21 cells, although is unable to detect their paralogs GAPDH1 and GAPDH3 (Figure 12, right panel).

Overproduction of three distinct functionally-active GAPDHs of *P. syringae* pv. tomato DC3000 in cell-free crude extracts of transformed BL21 clones was confirmed by enzymatic assays with nicotinamide coenzymes, both NAD^+ and $NADP^+$. As is shown in Table I, a phosphorlyating NAD^+-dependent dehydrogenase activity due to the native GapA, a typical glycolytic enzyme, was found at similar levels in both untransformed and pET21a-transformed *E. coli* BL-21 cells. Moreover, no significant $NADP^+$-dependent GAPDH activity was observed in these control clones. However, clear differences, both qualitative and quantitative, were observed in GAPDH specific activity levels of BL21 clones transformed with the pET21a-*gap* constructs. Thus, although the same phosphorylating NAD^+-dependent activity was found in BL-21 clones transformed with pET21a-*gap1* construct, a dramatic increase of specific activity (up to ca. 100-fold the control level) was determined for this overproducing clone. This should be due to the overproduction of *P. syringae* GAPDH1, which is a member of the glycolytic GAPDH family of cytoplasmic NAD^+-dependent enzymes (EC 1.2.1.12) involved in the glycolysis/pentoses-phosphate catabolic pathways in most bacteria and eukaryotes [42], as was shown previously in this work.

In contrast to that, cell extracts from BL-21 clones transformed with pET21a-*gap2* construct exhibit a comparative high level of phosphorylating $NADP^+$-dependent GAPDH activity (65-70 U/ml) besides a NAD^+-dependent activity level similar to those of control clones, due to the *E. coli* native enzyme. This should be due to overproduction of *P. syringae* GAPDH2 since *E. coli* does not possess any native $NADP^+$-dependent GAPDH. GAPDH2 is a member of a class I subfamily of $NADP^+$-dependent GAPDHs with 50-kDa subunits prevailing among gammaproteobacteria, but also present in other bacterial phylogenetic groups, as was previously shown in this work (see above). It was previously reported that the GAPDH2 ortholog GapB of the betaproteobacterium *Corynebacterium glutamicum* is an ATP-insensitive enzyme in contrast to its glycolytic GAPDH1 homolog, so these bacterial $NADP^+$-dependent GAPDHs have been proposed to be involved in anabolic gluconeogenic pathways [37]. In fact, they should be functionally equivalent enzymes to their $NAD(P)^+$-dependent cyanobacterial (EC 1.2.1.59) and chloroplastic (GapA/B, EC 1.2.1.13) counterparts of photosynthetic eukaryotes which are involved in the anabolic Calvin-Benson cycle [43,44], although they conform phylogenetically divergent subgroups of class I GAPDHs as was previously shown in this work (cf. Fig. 8).

However, the specific physiological role of *P. syringae* GAPDH2 and other gammabacterial 50-kDa orthologs remains to be determined and needs further research work.

On the other hand, cell extracts from BL-21 clones transformed with pET21a-*gap3* construct display a fairly high level (ca. 60 U/ml) of NAD^+-dependent GAPDH activity, 10-fold higher than control clones but still lower than the GAPDH1 overproducing clones, and no significant $NADP^+$-dependent activity. This result clearly indicates the presence of an overproduced NAD^+-dependent functional GAPDH besides the *E. coli* native enzyme. As previously discussed, the GAPDH encoded by *P. syringae gap3* is actually a member of a group bifunctional of erythrose-4-phosphate/glyceraldehyde-

3-phosphate dehydrogenase (EPD/GAPDH) enzymes, also called class III GAPDHs [11,45] which are substantially homologous to glycolytic GAPDH1-like enzymes, as was previously shown in this work. The EPD/GAPDH enzymes exhibit high non-phosphorylating erythrose-4-phosphate dehydrogenase activity and comparatively low phosphorylating NAD^+-dependent GADPH activity, hence the NAD^+-dependent activity level exhibited by the heterologously overproduced *P. syringae* GAPDH3, and its physiological role is not well understood yet. They have been found in many gammaproteobacteria (e.g. *E. coli*, *Vibrio cholerae*) [45], in some other proteobacterial groups, and remarkably in some parasitisc protists (*Giardia lamblia*) [46].

Overall, the obtained results indicate that the phytopathogenic gammaproteobacterium *P. syringae* pv. tomato DC3000 possess three enzymatically active GAPDHs of different catalytic features and distinct molecular phylogenies. The characterization of their physicochemical and catalytic properties, together with further comparative functional genomic studies, will help to clarify the precise physiological role of these important enzymes and its possible involvement in the infection process by this pathogenic bacterium.

Acknowledgments

This research was funded by the Programa de Cooperación Interuniversitaria e Investigación Científica of AECID (Agencia Española de Cooperación Internacional, MAEC, Spain) through the Collaborative Projects no. A1/043076/11 and A/030965/10. Also supported by the Moroccan CNRST (URAC). Partial support of BIO-261 group (PAIDI, Junta de Andalucia) is also acknowledged. IBVF is part of the CeiA3 and AndaluciaTech University Campuses of Scientific Excellence.

References

[1] N. Akesbi, Évolution et perspectives de l'agriculture marocaine, Rapport 50 Ans De Développement Humain Et Perspectives, 2025 (2006) 85–198.

[2] The Ministry of Agriculture and Maritime Fisheries of Morocco, Moroccan agriculture in number, (2010).

[3] Y. Bashan, L.E. De-Bashan, Protection of tomato seedlings against infection by *Pseudomonas syringae* pv tomato by using the plant growth-promoting bacterium Azospirillum brasilense, Applied and Environmental Microbiology, 68 (2002) 2637–2643.

[4] A. Rico, G.M. Preston, *Pseudomonas syringae* pv tomato DC3000 uses constitutive and apoplast-induced nutrient assimilation pathways to catabolize nutrients that are abundant in the tomato apoplast, Molecular Plant-microbe Interactions, 21 (2008) 269–282.

[5] H. Feil, W.S. Feil, P. Chain, F. Larimer, G. DiBartolo, A. Copeland, A. Lykidis, S. Trong, M. Nolan, E. Goltsman, Comparison of the complete genome sequences of *Pseudomonas syringae* pv syringae B728a and pv tomato DC3000, Proceedings of the National Academy of Sciences of the United States of America, 102 (2005) 11064–11069.

[6] D.E. Fouts, R.B. Abramovitch, J.R. Alfano, A.M. Baldo, C.R. Buell, S. Cartinhour, A.K. Chatterjee, M. D'Ascenzo, M.L. Gwinn, S.G. Lazarowitz, Genomewide identification of *Pseudomonas syringae* pv tomato DC3000 promoters controlled by the HrpL alternative sigma factor, Proceedings of the National Academy of Sciences, 99 (2002) 2275–2280.

[7] C.R. Buell, V. Joardar, M. Lindeberg, J. Selengut, I.T. Paulsen, M.L. Gwinn, R.J. Dodson, R.T. Deboy, A.S. Durkin, J.F. Kolonay, The complete genome sequence of the Arabidopsis and tomato pathogen *Pseudomonas syringae* pv tomato DC3000, Proceedings of the National Academy of Sciences, 100 (2003) 10181–10186.

[8] A. Pérez-García, F.M. Cánovas, F. Gallardo, B. Hirel, A. Vicente, Differential expression of glutamine synthetase isoforms in tomato detached leaflets infected with *Pseudomonas syringae* pv tomato, MPMI-Molecular Plant Microbe Interactions, 8 (1995) 96–103.

[9] D.A. Cuppels, J. Elmhirst, Disease development and changes in the natural *Pseudomonas syringae* pv tomato populations on field tomato plants, Plant Disease, 83 (1999) 759–764.

[10] A. Soukri, F. Valverde, N. Hafid, M.S. Elkebbaj, A. Serrano, Occurrence of a differential expression of the glyceraldehyde-3-phosphate dehydrogenase gene in muscle and liver from euthermic and induced hibernating jerboa (*Jaculus orientalis*), Gene, 181 (1996) 139–145.

[11] R.M. Figge, M. Schubert, H. Brinkmann, R. Cerff, Glyceraldehyde-3-phosphate dehydrogenase gene diversity in eubacteria and eukaryotes: evidence for intra- and inter-kingdom gene transfer, Molecular Biology and Evolution, 16 (1999) 429–440.

[12] A. Soukri, F. Valverde, N. Hafid, M.S. Elkebbaj, A. Serrano, Characterization of muscle glyceraldehyde-3-phosphate dehydrogenase isoforms from euthermic and induced hibernating *Jaculus orientalis*, Biochimica Et Biophysica Acta (BBA)-General Subjects, 1243 (1995) 161–168.

[13] J. Petersen, H. Brinkmann, R. Cerff, Origin, Evolution and Metabolic Role of a Novel Glycolytic GAPDH Enzyme Recruited by Land Plant Plastids, J Mol Evol, 57 (2003) 16–26.

[14] A. Habenicht, The non-phosphorylating glyceraldehyde-3-phosphate dehydrogenase: biochemistry, structure, occurrence and evolution, Biological Chemistry, 78 (1997) 1413-1419.

[15] K. Meyer-Siegler, D.J. Mauro, G. Seal, J. Wurzer, J.K. deRiel, M.A. Sirover, A human nuclear uracil DNA glycosylase is the 37-kDa subunit of glyceraldehyde-3-phosphate dehydrogenase, PNAS, 88 (1991) 8460–8464.

[16] L. Barbini, J. Rodríguez, F. Dominguez, F. Vega, Glyceraldehyde-3-phosphate dehydrogenase exerts different biologic activities in apoptotic and proliferating hepatocytes according to its subcellular localization, Molecular and Cellular Biochemistry, 300 (2007) 19–28.

[17] M.A. Sirover, New insights into an old protein: the functional diversity of mammalian glyceraldehyde-3-phosphate dehydrogenase, Biochimica Et Biophysica Acta (BBA)-Protein Structure and Molecular Enzymology, 1432 (1999) 159–184.

[18] L. Zheng, R.G. Roeder, Y. Luo, S Phase Activation of the Histone H2B Promoter by OCA-S, a Coactivator Complex that Contains GAPDH as a Key Component, Cell, 114 (2003) 255–266.

[19] M. Engel, M. Seifert, B. Theisinger, U. Seyfert, C. Welter, Glyceraldehyde-3-phosphate Dehydrogenase and Nm23-H1/Nucleoside Diphosphate Kinase A TWO OLD ENZYMES COMBINE FOR THE NOVEL Nm23 PROTEIN PHOSPHOTRANSFERASE FUNCTION, J. Biol. Chem., 273 (1998) 20058–20065.

[20] D.A. Butterfield, S.S. Hardas, M.L.B. Lange, Oxidatively modified glyceraldehyde-3-phosphate dehydrogenase (GAPDH) and Alzheimer's disease: many pathways to neurodegeneration, Journal of Alzheimer's Disease, 20 (2010) 369–393.

[21] J.R. Burke, J.J. Enghild, M.E. Martin, Y.S. Jou, R.M. Myers, A.D. Roses, J.M. Vance, W.J. Strittmatter, Huntingtin and DRPLA proteins selectively interact with the enzyme GAPDH, Nature Medicine, 2 (1996) 347–350.

[22] M. Citron, T. Oltersdorf, C. Haass, L. McConlogue, A.Y. Hung, P. Seubert, C. Vigo-Pelfrey, I. Lieberburg, D.J. Selkoe, Mutation of the β-amyloid precursor protein in familial Alzheimer's disease

increases β-protein production, , Published Online: 17 December 1992; | Doi:10.1038/360672a0, 360 (1992) 672–674.

[23] P.E. Glaser, R.W. Gross, Rapid Plasmenylethanolamine-Selective Fusion of Membrane Bilayers Catalyzed by an Isoform of Glyceraldehyde-3-Phosphate Dehydrogenase: Discrimination between Glycolytic and Fusogenic Roles of Individual Isoforms, Biochemistry, 34 (1995) 12193–12203.

[24] T. Nakagawa, Y. Hirano, A. Inomata, S. Yokota, K. Miyachi, M. Kaneda, M. Umeda, K. Furukawa, S. Omata, T. Horigome, Participation of a Fusogenic Protein, Glyceraldehyde-3-phosphate Dehydrogenase, in Nuclear Membrane Assembly, J. Biol. Chem., 278 (2003) 20395–20404.

[25] , J. Renau-Piqueras, M.L. Gil, D. Gozalbo, The glyceraldehyde-3-phosphate dehydrogenase polypeptides encoded by the *Saccharomyces cerevisiae* TDH1, TDH2 and TDH3 genes are also cell wall proteins, Microbiology, 147 (2001) 411–417.

[26] K. Dheda, J.F. Huggett, S.A. Bustin, M.A. Johnson, G. Rook, A. Zumla, Validation of housekeeping genes for normalizing RNA expression in real-time PCR, Biotechniques, 37 (2004) 112–119.

[27] A.H. Alvarez, G. Martinez-Cadena, M.E. Silva, E. Saavedra, E.E. Avila, *Entamoeba histolytica*: ADP-ribosylation of secreted glyceraldehyde-3-phosphate dehydrogenase, Experimental Parasitology, 117 (2007) 349–356.

[28] B. Kenny, B.B. Finlay, Protein secretion by enteropathogenic *Escherichia coli* is essential for transducing signals to epithelial cells, Proceedings of the National Academy of Sciences, 92 (1995) 7991–7995.

[29] L. Aguilera, E. Ferreira, R. Giménez, F.J. Fernández, M. Taulés, J. Aguilar, M.C. Vega, J. Badia, L. Baldomà, Secretion of the housekeeping protein glyceraldehyde-3-phosphate dehydrogenase by the LEE-encoded type III secretion system in enteropathogenic *Escherichia coli*, Int. J. Biochem. Cell Biol., 44 (2012) 955–962.

[30] Z. Eichenbaum, B.D. Green, J.R. Scott, Iron starvation causes release from the group A streptococcus of the ADP-ribosylating protein called plasmin receptor or surface glyceraldehyde-3-phosphate-dehydrogenase, Infection and Immunity, 64 (1996) 1956–1960.

[31] V. Pancholi, V.A. Fischetti, Regulation of the phosphorylation of human pharyngeal cell proteins by group A streptococcal surface dehydrogenase: signal transduction between streptococci and pharyngeal cells, The Journal of Experimental Medicine, 186 (1997) 1633–1643.

[32] T. Maniatis, Molecular cloning: a laboratory manual/J Sambrook, EF Fritsch, T Maniatis, New York: Cold Spring Harbor Laboratory Press, 1989.

[33] A. BradfordMM, rapid and sensitive method for the quantitation of microgram quantities of protein utilizing the principle of protein–dye binding, Anal Biochem, 72 (1976) 248–254.

[34] U.K. Laemmli, Cleavage of structural proteins during the assembly of the head of bacteriophage T4, Nature, 227 (1970) 680–685.

[35] A. Iddar, A. Serrano, A. Soukri, A phosphate-stimulated NAD (P)+-dependent glyceraldehyde-3-phosphate dehydrogenase in *Bacillus cereus*, FEMS Microbiology Letters, 211 (2002) 29–35.

[36] A.H. Alvarez, G. Martinez-Cadena, M.E. Silva, E. Saavedra, E.E. Avila, *Entamoeba histolytica*: ADP-ribosylation of secreted glyceraldehyde-3-phosphate dehydrogenase, Experimental Parasitology, 117 (2007) 349–356.

[37] C.A. Omumasaba, N. Okai, M. Inui, H. Yukawa, *Corynebacterium glutamicum* Glyceraldehyde-3-Phosphate Dehydrogenase Isoforms with Opposite, ATP-Dependent Regulation, Journal of Molecular Microbiology and Biotechnology, 8 (2004) 91–103.

[38] R.M. Figge, M. Schubert, H. Brinkmann, R. Cerff, Glyceraldehyde-3-phosphate dehydrogenase gene diversity in eubacteria and eukaryotes: evidence for intra-and inter-kingdom gene transfer, Molecular Biology and Evolution, 16 (1999) 429–440.

[39] V. Bardey, C. Vallet, N. Robas, B. Charpentier, B. Thouvenot, A. Mougin, E. Hajnsdorf, P. Régnier, M. Springer, C. Branlant, Characterization of the molecular mechanisms involved in the differential production of erythrose-4-phosphate dehydrogenase, 3-phosphoglycerate kinase and class II fructose-1, 6-bisphosphate aldolase in Escherichia coli, Molecular Microbiology, 57 (2005) 1265–1287.

[40] F. Saida, M. Uzan, B. Odaert, F. Bontems, Expression of highly toxic genes in E coli: special strategies and genetic tools, Current Protein and Peptide Science, 7 (2006) 47–56.

[41] N. Hafid, F. Valverde, E. Villalobo, M.S. Elkebbaj, A. Torres, A. Soukri, A. Serrano, Glyceraldehyde-3-phosphate dehydrogenase from *Tetrahymena pyriformis*: enzyme purification and characterization of a *gapC* gene with primitive eukaryotic features, Comparative Biochemistry and Physiology Part B: Biochemistry and Molecular Biology, 119 (1998) 493–503.

[42] P.D. Boyer, The Enzymes, Academic Press, 1976.

[43] F. Valverde, M. Losada, A. Serrano, Functional complementation of an Escherichia coli gap mutant supports an amphibolic role for NAD (P)-dependent glyceraldehyde-3-phosphate dehydrogenase of Synechocystis sp strain PCC 6803, Journal of Bacteriology, 179 (1997) 4513–4522.

[44] G. Ferri, G. Comerio, P. Ladarola, M.C. Zapponi, M.L. Speranza, Subunit structure and activity of glyceraldehyde-3-phosphate dehydrogenase from spinach chloroplasts, Biochimica Et Biophysica Acta (BBA)-Enzymology, 522 (1978) 19–31.

[45] G. Zhao, A.J. Pease, N. Bharani, M.E. Winkler, Biochemical characterization of gapB-encoded erythrose 4-phosphate dehydrogenase of *Escherichia coli* K-12 and its possible role in pyridoxal 5'-phosphate biosynthesis, Journal of Bacteriology, 177 (1995) 2804–2812.

[46] P.R. Alefounder, R.N. Perham, Identification, molecular cloning and sequence analysis of a gene cluster encoding the Class II fructose 1, 6-bisphosphate aldolase, 3-phosphoglycerate kinase and a putative second glyceraldehyde 3-phosphate dehydrogenase of *Escherichia coli*, Molecular Microbiology, 3 (2006) 723–732.

Figures Legends:

Figure 1. Domain architecture of the class I glyceraldehyde 3-phosphate dehydrogenase protein encoded by the *gap1* gene of *Pseudomonas syringae* pv. tomato str. DC3000 (**gi|28868497|ref|NP_791116.1|**), as predicted by ProDom (top), SUPERFAMILY (middle) and Pfam (bottom) bioinformatics tools.

Figure 2. Structure of the genomic region (ca. 20 kb) around the *gap1* gene of *P. syringae* pv. tomato DC3000. Sequence data were from the Pseudomonas Genome Database (top) and JGI microbial genomes (bottom) websites. Gene designation of indicated ORFs is based on the closest BLAST hit. Note that adjacent divergent genes *gap1* and *edd* arrange in a head-to-head manner in opposite orientations.

Figure 3. Domain architecture of the class I glyceraldehyde 3-phosphate dehydrogenase protein (GAPDH2, 482 aa) encoded by the *gap2* gene of *Pseudomonas syringae* pv. tomato str. DC3000 (**gi|28869306|ref|NP_791925.1|**), as predicted by ProDom (top), SUPERFAMILY (middle) and Pfam (bottom) bioinformatics tools. Note the N-terminal extra region of ca. 130 aminoacids upstream the GAPDH-specific domains.

Figure 4. Structure of the genomic region (ca. 20 kb) around the *gap2* gene of *P. syringae* pv. tomato DC3000. Sequence data were from the Pseudomonas Genome Database (top) and JGI microbial genomes (bottom) websites. Gene designation of indicated ORFs is based on the closest BLAST hit. Note that adjacent divergent genes *gap2* and *mfd* arrange in a head-to-head manner in opposite orientations.

Figure 5. Domain architecture of the putative class III glyceraldehyde 3-phosphate dehydrogenase protein (GAPDH3, 347 aa) encoded by the *gap3* gene of *Pseudomonas syringae* pv. tomato str. DC3000 (gi|28867616|ref|NP_790235.1), as predicted by ProDom (top), SUPERFAMILY (middle) and Pfam (bottom) bioinformatics tools. This protein belongs to a group of bifunctional D-erythrose 4-phosphate dehydrogenase/GAPDH enzymes prevailing among gammaproteobacteria.

Figure 6. Structure of the genomic region (ca. 20 kb) around the *gap3/epd* gene of *P. syringae* pv. tomato DC3000. Sequence data were from the Pseudomonas Genome Database (top) and JGI microbial genomes (bottom) websites. Gene designation of indicated ORFs is based on the closest BLAST hit. Note the occurrence of *gap3* gene in an operon with other genes encoding glycolysis/pentoses phosphate pathway enzymes (*tkt*, *pgk* and *fba*).

Figure 7. Multiple sequence alignment of the three GAPDHs of *P. syringae* pv. tomato DC3000 and selected prototypical orthologs of class I (*E. coli* GapA and *Corynebacterium glutamicum* GapB) and class III (*E. coli* GapB-Epd) GAPDHs. Alignment of aminoacid sequences was performed with ClustalX software. Shadowing displaying fully conserved positions in black and conservative changes in gray was made with Boxshade v 3.3 (http://mobyle.pasteur.fr/cgi-bin/portal.py?#forms::boxshade). The essential Cys residue that directly participates in the catalytic mechanism (thiohemiacetal/thioester intermediate with substrate) is marked with an asterisk.

Figure 8. Molecular phylogenetic analysis of the three GAPDHs of *P. syringae* pv. tomato DC3000. Full amino acid sequences derived from the paralogous *gap* genes studied in this work were aligned with selected sequences of class I and class III GAPDHs of other bacteria and eukaryotes using CLUSTAL X program, and then subjected to phylogenetic analysis by distance (Neighborg-Joining) method with the MEGA4 program. Possible clusters of functional equivalent orthologs of class I and class III GAPDHs are presented. Biochemical characterized enzymes are boxed and the three bacterial paralogs studied in this work are marked with arrows. Numbers in nodes indicate the statistical support (bootstrap values for 1000 replicates) of selected clusters of homologs. The bar represents amino acid substitutions per site.

Figure 9. Electrophoretic analysis of PCR-amplified DNA fragments corresponding to the three *gap* genes of *P. syringae* pv. tomato DC3000. Amplifications were performed with specific primers pairs and bacterial genomic DNA as a template, as described in Material and Methods, and subsequently loaded onto 1% agarose-TBE gels using EcoRI/HindIII-cleaved lambda phage DNA as a marker (M). Single DNA bands of ca. 1.5, 1.1 and 1.0 kb obtained in four independent PCR experiments for *gap3* (1,446 bp), *gap2* (1,041 bp) and *gap1* (999 bp), respectively, are shown.

Figure 10. Coomassie blue stained SDS–PAGE electrophoretogram showing the protein patterns of cell-free extracts (ca. 50 µg protein per lane) from *E. coli* BL21 transformed clones. Overproduction of the three GAPDHs from *P. syringae* was achieved under different conditions of induction. The molecular masses of protein markers (M) are shown on the left. Arrows with the expected molecular masses of GAPDH subunits on the right side indicate the band positions of overproduced proteins. Lane 1: BL-21 transformed with pET21a-*gap1* construct after 4 h of IPTG induction; lane 2: BL-21 transformed with pET21a-*gap1* construct after overnight IPTG induction; lane 3: BL-21 transformed with pET21a-*gap2* construct after 4 h of IPTG induction; lane 4: BL-21 transformed with pET21a-*gap2* construct after overnight IPTG induction; lane 5: BL-21 transformed with pET21a-*gap3* construct after 4 h of IPTG induction at 22 ºC; lane 6: BL-21 transformed with pET21a-*gap3* construct after overnight IPTG induction at 22 ºC; lane 7: BL-21 transformed with plasmid pET21a without insert and after overnight IPTG induction; lane 8: not transformed BL-21 cells.

Figure 11. Effect of alternative carbon sources on the overproduction levels of *P. syringae* pv. tomato DC3000 GAPDH1 and GAPDH2 in *E. coli* BL21 cells. SDS-PAGE analysis of cell-free extracts (ca. 50 µg protein per lane) from *E. coli* BL21 transformed clones grown in LB medium supplemented with succinate, glycerol, succinate *plus* glycerol or glucose is shown. Induction was carried out with IPTG, as described in the text. NA: no alternative carbon source added, used as control cultures.

Figure 12. Immunoblot analysis of cell-free extracts from *E. coli* BL21 transformed clones overproducing the three GAPDHs of *P. syringae* pv. tomato DC3000 strain. **Left panel:** immunodetection of recombinant GAPDH1 and GAPDH3 using monospecific antibodies against the GAPDH GapC of the protist *Tetrahymena pyriformis* [41]. **Right panel:** immunodetection of recombinant GAPDH2 with monospecific polyclonal antibodies against the GAPDH2 of *P. syringae* pv. tomato DC3000. Lanes 1 and 4: BL-21 transformed with pET21a-*gap2* construct after 4 h of IPTG induction; lane 2: BL-21 transformed with pET21a-*gap3* construct after 4 h of IPTG induction at 22 ºC; lane 3: BL-21 transformed with pET21a-*gap1* construct after overnight IPTG induction; lane 5: BL-21 transformed with pET21a-*gap2* construct after 4 h of IPTG induction; lane 6: BL-21 transformed with pET21a-*gap1* construct after overnight IPTG induction; lane 7: BL-21 transformed with pET21a-*gap3* construct after 4 h of IPTG induction at 22 ºC. About 50 µg of protein were loaded per lane and transferred to nitrocellulose membrane after SDS-PAGE. The molecular masses of pre-stained protein markers (M) are shown on the left of each panel. The expected molecular masses of GAPDH subunits are shown on the right side of arrows indicating the positions of the immunodetected bands of overproduced proteins.

Tables

Table 1. Complementary primers used for PCR amplifications of P. syringae gap genes

Gene	Primers (new restriction site, underlined)	
gap1 Pseudomonas syringae pv tomatoDC3000	F (*Nde*I)	5'-GGAATTCCATATGACTCTCCGTATCGCAATC-3'
	R (*Bam*H1)	5'-CGGGATCCTTACTCGGCGTTATGCAGCGC-3'
gap2 Pseudomonas syringae pv. tomato DC3000	F (*Nde*I)	5'-GGAATTCCATATGACTCAGAAGCCCGACCAG-3'
	R (*Hind*III)	5'-CCCAAGCTTTTACTGCGGGAACGCTGGCGG-3'
gap3/epd Pseudomonas syringae pv. tomato DC3000	F (*Nde*I)	5'-GGAATTCCATATGCCCCAGCCCCGCCCTTAC-3'
	R (*Bam*H1)	5'-CGGGATCCTTATTGGTCAGCGACGCGCAA-3'

Table 2. Glyceraldehyde-3-phosphate dehydrogenase enzymatic activity levels with nicotinamide nucleotide coenzymes in cell-free extracts of transformed *E. coli* BL21 cells

E. coli strain	*P. syringae* recombinant gene	GAPDH activity (U mg^{-1})[a]	
		NAD^+	$NADP^+$
BL21		0.60 ± 0.04	≤ 0.01
BL21 Transformed, not induced		0.66 ± 0.06	≤ 0.01
BL21 Transformed and induced	*gap1*	74.28 ± 0,02	≤ 0.01
	gap2	0.78 ± 0.07	10.80± 0.10
	gap3	7.35 ± 0.14	≤ 0.01

[a] Means and standard errors of three independent determinations of activity levels, carried out in cell crude extracts (soluble protein fraction), are shown.

Figure

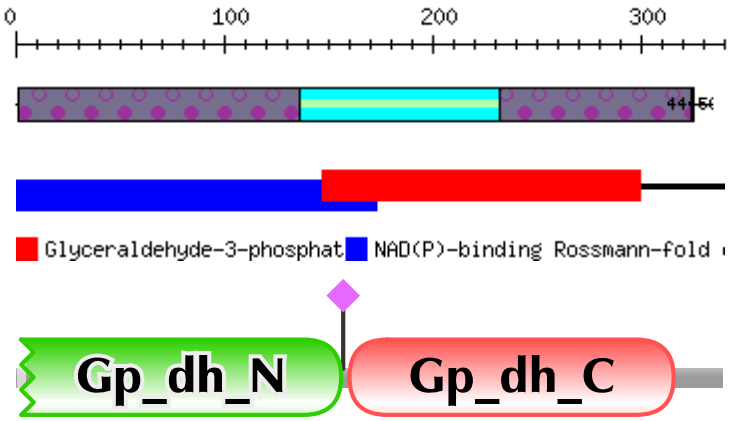
0
100
200
300
Glyceraldehyde-3-phosphat
NAD(P)-binding Rossmann-fold
Gp_dh_N
Gp_dh_C

Fig. 1

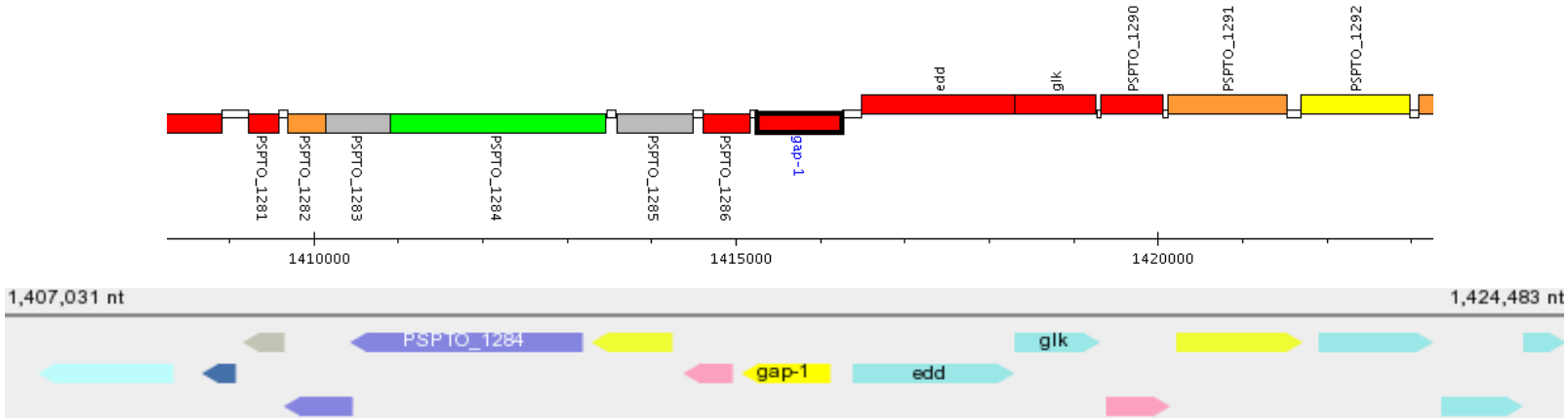
edd
glk
PSPTO_1290
PSPTO_1291
PSPTO_1292
PSPTO_1281
PSPTO_1282
PSPTO_1283
PSPTO_1284
PSPTO_1285
PSPTO_1286
gap-1
1410000
1415000
1420000
1,407,031 nt
1,424,483 nt
PSPTO_1284
glk
gap-1
edd

Fig. 2

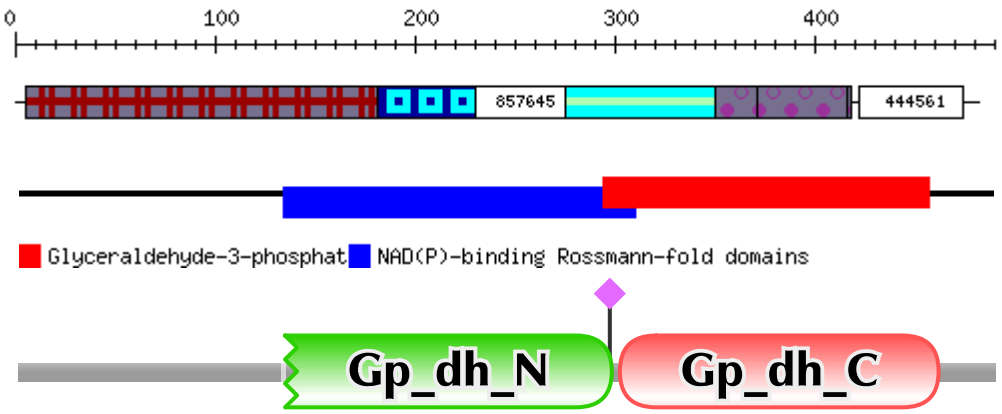
0
100
200
300
400
857645
444561
Glyceraldehyde-3-phosphat
NAD(P)-binding Rossmann-fold domains
Gp_dh_N
Gp_dh_C

Fig. 3

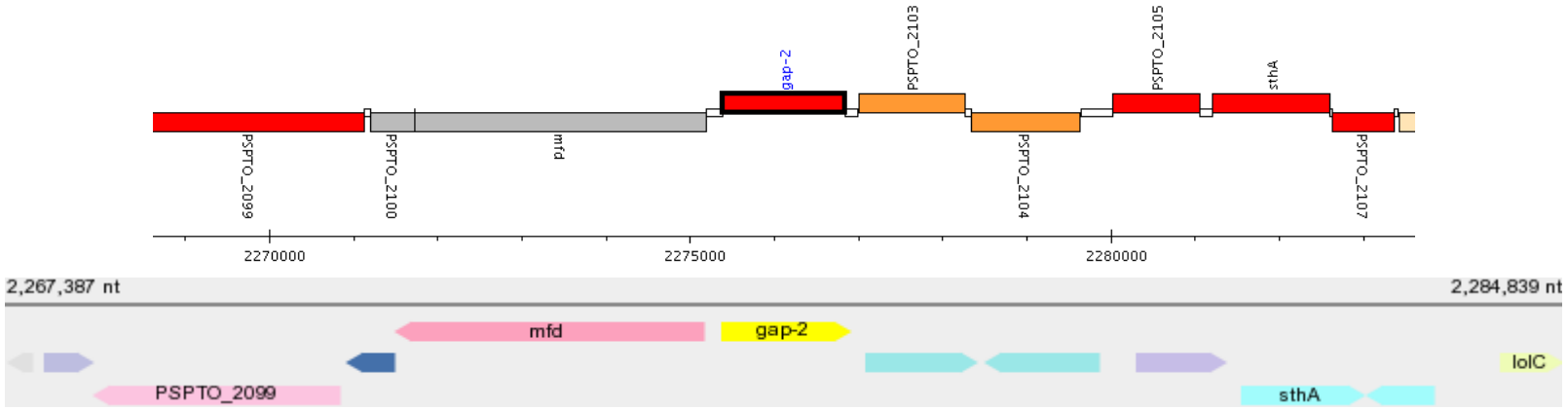
gap-2
PSPTO_2103
PSPTO_2105
sthA
PSPTO_2099
PSPTO_2100
mfd
PSPTO_2104
PSPTO_2107
2270000
2275000
2280000
2,267,387 nt
2,284,839 nt
mfd
gap-2
lolC
PSPTO_2099
sthA

Fig. 4

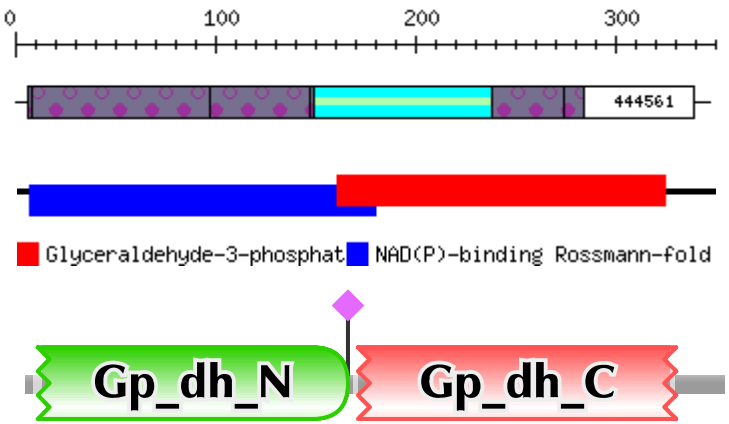
0
100
200
300
444561
Glyceraldehyde-3-phosphat
NAD(P)-binding Rossmann-fold
Gp_dh_N
Gp_dh_C

Fig. 5

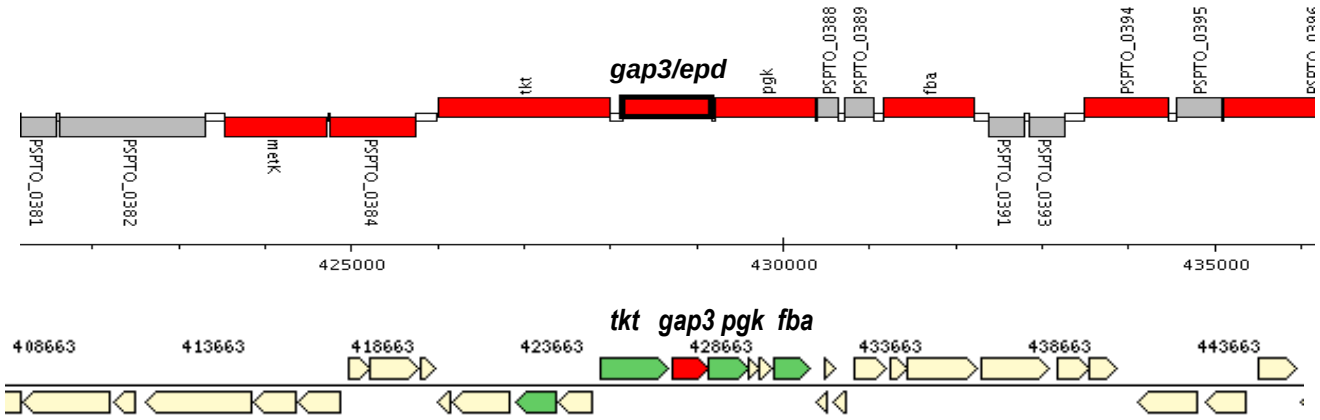
gap3/epd
tkt
pgk
PSPTO_0388
PSPTO_0389
fba
PSPTO_0394
PSPTO_0395
PSPTO_0381
PSPTO_0382
metK
PSPTO_0384
PSPTO_0391
PSPTO_0393
425000
430000
435000
tkt gap3 pgk fba
408663
413663
418663
423663
428663
433663
438663
443663

Fig. 6


>Q887K5_PSESM GAPDH1
>P0A9B2_ECOLI GapA
>Q884J0_PSESM GAPDH2
>Q2XUQ9_CORGT GapB
>Q88AK4_PSESM GAPDH3-EPD
>P0A9B6_ECOLI GapB-Epd

Fig. 7

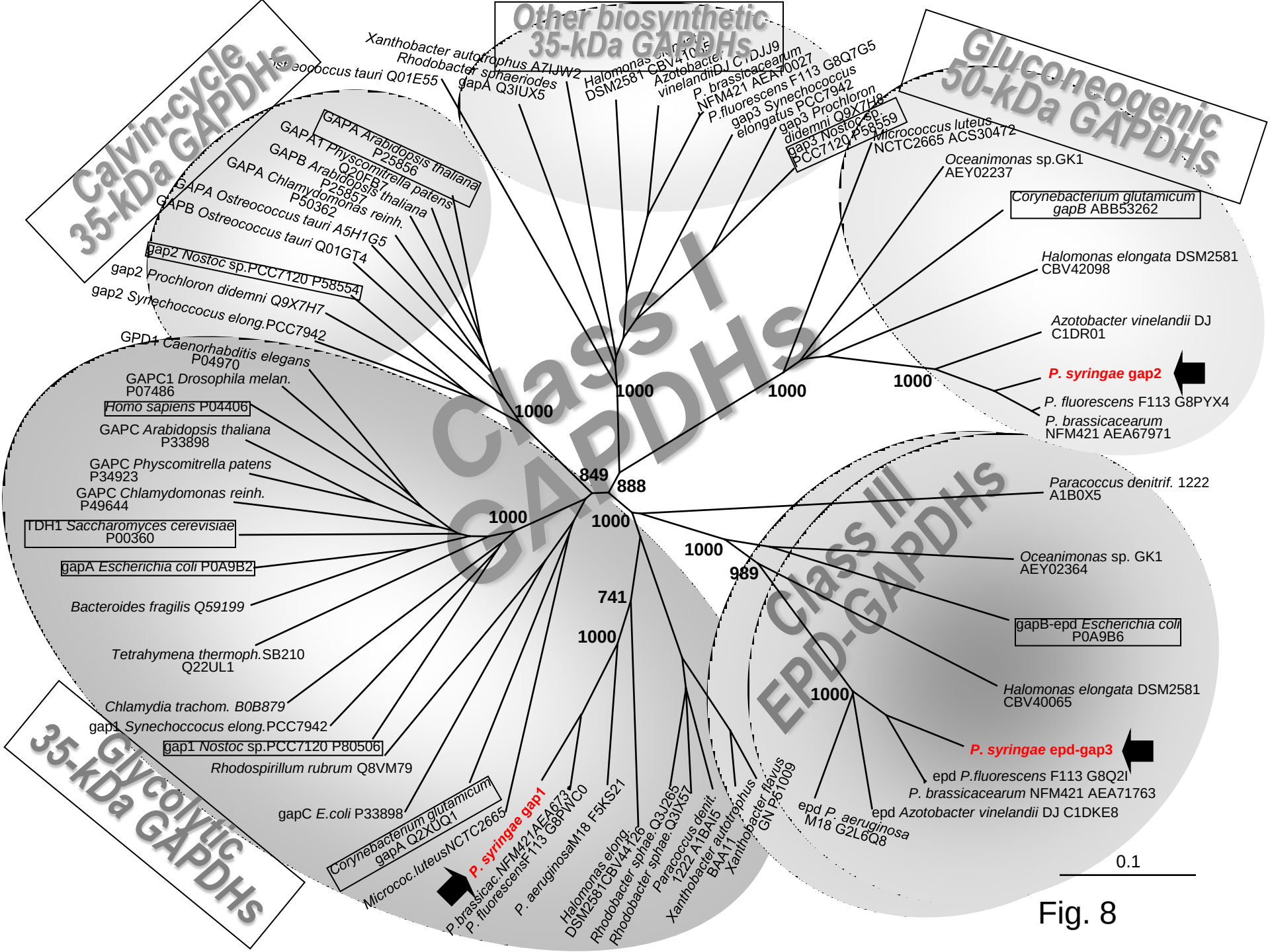
Calvin-cycle 35-kDa GAPDHs
Other biosynthetic 35-kDa GAPDHs
Gluconeogenic 50-kDa GAPDHs
Class I GAPDHs
Class III EPD-GAPDHs
Glycolytic 35-kDa GAPDHs
Xanthobacter autotrophus A7IJW2
Rhodobacter sphaeriodes gapA Q3IUX5
Halomonas elong. DSM2581 CBV42100
Azotobacter vinelandii DJ C1DJJ9
P. brassicacearum NFM421 AEA70027
P.fluorescens F113 G8Q7G5
gap3 Synechococcus elongatus PCC7942
gap3 Prochloron didemni Q9X7H8
gap3 Nostoc sp. PCC7120 P58559
Micrococcus luteus NCTC2665 ACS30472
Oceanimonas sp.GK1 AEY02237
Corynebacterium glutamicum gapB ABB53262
Halomonas elongata DSM2581 CBV42098
Azotobacter vinelandii DJ C1DR01
P. syringae gap2
P. fluorescens F113 G8PYX4
P. brassicacearum NFM421 AEA67971
Paracoccus denitrif. 1222 A1B0X5
Oceanimonas sp. GK1 AEY02364
gapB-epd Escherichia coli P0A9B6
Halomonas elongata DSM2581 CBV40065
P. syringae epd-gap3
epd P.fluorescens F113 G8Q2I
P. brassicacearum NFM421 AEA71763
epd Azotobacter vinelandii DJ C1DKE8
epd P. aeruginosa M18 G2L6Q8
Xanthobacter flavus GNP51009
Xanthobacter autotrophus BAA11
Paracoccus denit. 1222 A1BAI5
Rhodobacter sphae. Q3IX57
Rhodobacter sphae. Q3J265
Halomonas elong. DSM2581CBV44126
P. aeruginosaM18 F5KS21
P. fluorescensF113 G8PWC0
P.brassicac.NFM421AEA673
P. syringae gap1
Micrococ.luteusNCTC2665
Corynebacterium glutamicum gapA Q2XUQ1
gapC E.coli P33898
Rhodospirillum rubrum Q8VM79
gap1 Nostoc sp.PCC7120 P80506
gap1 Synechoccocus elong.PCC7942
Chlamydia trachom. B0B879
Tetrahymena thermoph.SB210 Q22UL1
Bacteroides fragilis Q59199
gapA Escherichia coli P0A9B2
TDH1 Saccharomyces cerevisiae P00360
GAPC Chlamydomonas reinh. P49644
GAPC Physcomitrella patens P34923
GAPC Arabidopsis thaliana P33898
Homo sapiens P04406
GAPC1 Drosophila melan. P07486
GPD1 Caenorhabditis elegans P04970
gap2 Synechoccocus elong.PCC7942
gap2 Prochloron didemni Q9X7H7
gap2 Nostoc sp.PCC7120 P58554
GAPB Ostreococcus tauri Q01GT4
GAPA Ostreococcus tauri A5H1G5
GAPB Chlamydomonas reinh. P25857
GAPB Arabidopsis thaliana Q20FB7
GAPA1 Physcomitrella patens P25856
GAPA Arabidopsis thaliana P25856
Ostreococcus tauri Q01E55
1000
1000
1000
849
888
1000
1000
1000
989
741
1000
1000
0.1

Fig. 8

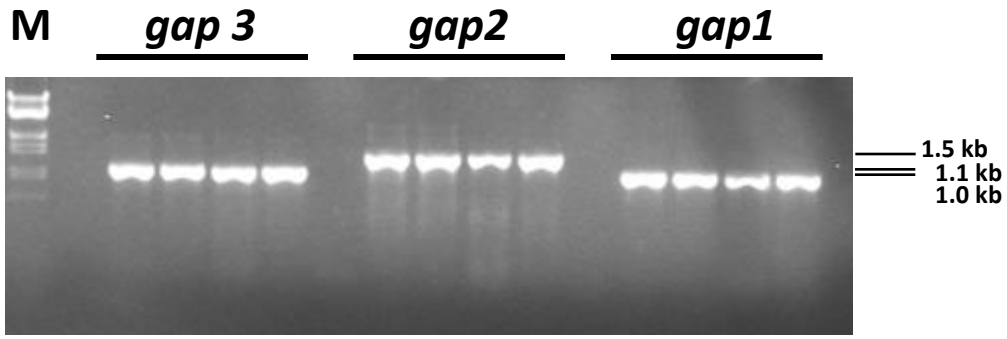

Fig. 9

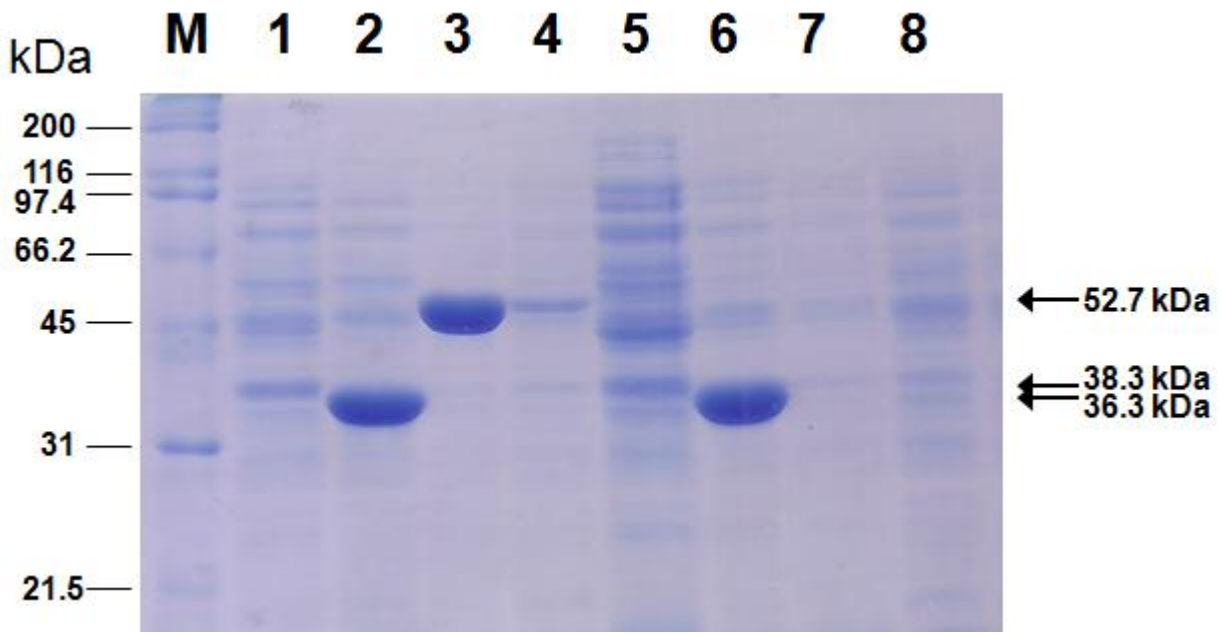

Fig. 10

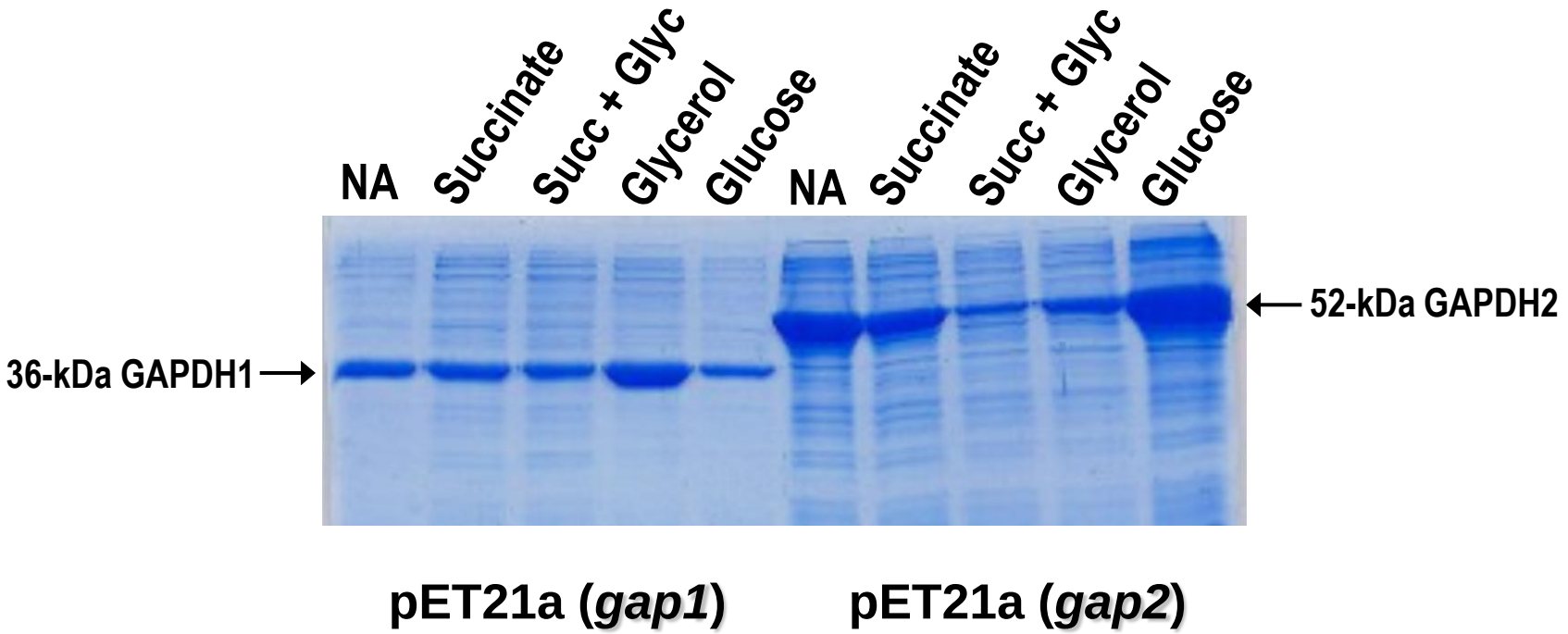
NA
Succinate
Succ + Glyc
Glycerol
Glucose
NA
Succinate
Succ + Glyc
Glycerol
Glucose
36-kDa GAPDH1
52-kDa GAPDH2
pET21a (gap1)
pET21a (gap2)

Fig. 11

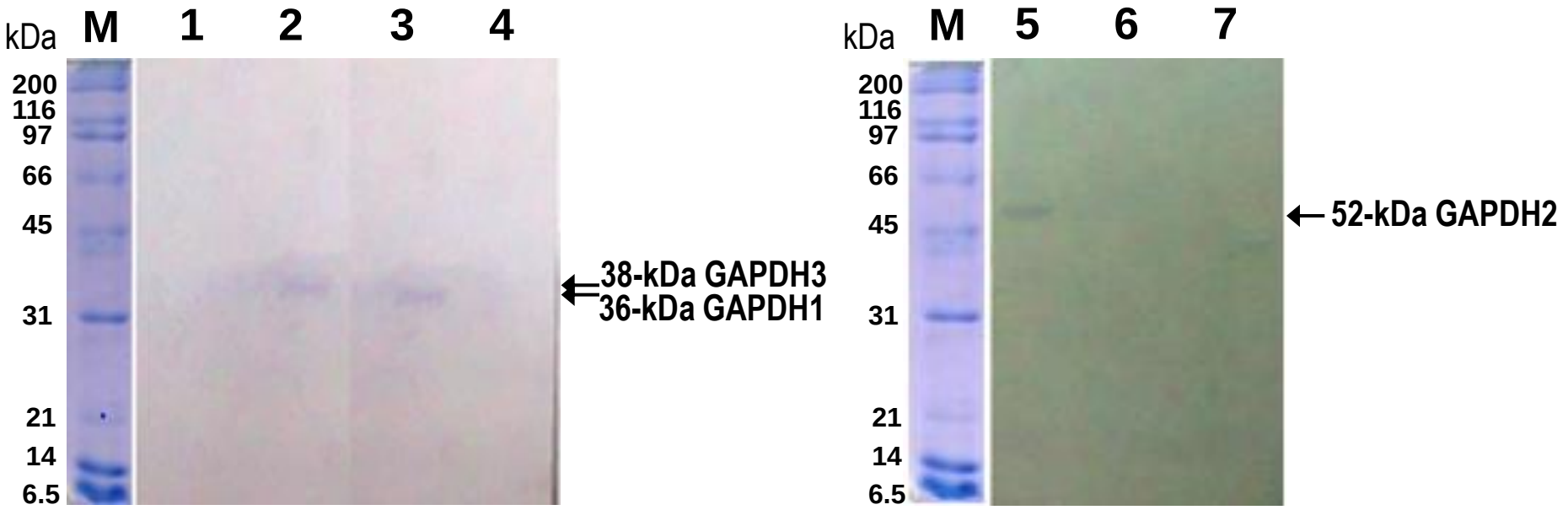
kDa
M
1
2
3
4
200
116
97
66
45
31
21
14
6.5
38-kDa GAPDH3
36-kDa GAPDH1
kDa
M
5
6
7
200
116
97
66
45
31
21
14
6.5
52-kDa GAPDH2

Fig. 12